Numerical solution of a 2D lubrication model with Sommerfeld boundary conditions for hip prostheses

B.A. Weiss, M.E. Berli, S. Ubal and J. Di Paolo

Grupo Biomecánica Computacional, Facultad de Ingeniería, Universidad Nacional de Entre Ríos, Oro Verde, Argentina

Abstract— **Prosthetic in-contact surfaces wear is one of the main causes of hip replacements failure. Lubrication is essential to reduce the friction and consequently the wear. A two-dimensional model based on a modified Reynolds equation, was used to analyze the lubricated contact in a hypothetical hip prosthesis. It is assumed that prosthesis is made of a metallic component and a low rigidity elastic porous material that can absorb or exude fluid. The fluid pressure and channel flow shape were simultaneously solved by a double precision computer code based on the finite element method, Newton's method and parametric continuation.**

The information provided by this model is extremely difficult to obtain by experimental methods. Results show that a greater deformation capacity of the elastic material promotes a thicker lubrication film and induces a better load distribution reducing normal stresses; while exudation capacity reduces friction and wear. The sub-ambient pressures predicted and the oscillatory solution, show the need of more realistic boundary conditions and finite element mesh refinement.

Keywords— **Hip prosthesis, poro-elasto-hydrodynamic lubrication, friction, wear.**

I. Introduction

The average lifespan of hip prostheses is about 15 years, after that, new surgeries (revisions) and psychophysical disorders in young people can arise [1]. One of the main causes of prostheses failure is ultra high molecular weight polyethylene (UHMWPE) wear [2]. In addition, significant increases in the number of hip arthroplasties and revisions are foreseen [1], which motivates the study of the lubricated contact, since this is a key factor to reduce the friction between surfaces and consequently to reduce wear.

The bones that form the natural hip joint are coated with hyaline cartilage, this is a deformable porous material formed by a network of hydrophilic molecules that allow it to maintain a high degree of hydration. Cartilage exudes or absorbs liquid when it is compressed or expanded, respectively. This behavior is essential for the operation with low coefficients of friction in healthy joints, besides it promotes a self-lubricating mechanism [3].

One-dimensional lubrication models (e.g. [4]) of a hypothetical prosthesis made of a metallic component and an elastic porous material showed a decrease of the friction coefficient by up to 30%. In this work a two-dimensional poro-elasto-hydrodynamic lubrication model is solved by means of an algorithm based on the finite element method.

II. Materials and Methods

A. Characteristics of the model

In the lubricated contact area, the convex femoral prosthetic surface is assumed as a spherical surface in-contact with a concave spherical surface that represents the acetabular component. In this geometrical approximation, named point contact model [1], the equivalent radius (R) of the sphere is such that its curvature is equal to the difference between the curvatures of the original elements.

The model equations are obtained assuming the following hypotheses:

1. Lubrication approximation.
2. Incompressible Newtonian synovial fluid.
3. Steady state, bidirectional, laminar and Couette dominant flow.
4. Non-deformable femoral component.
5. Low rigidity and porous acetabular component, capable of exuding or absorbing fluid.
6. Constant elastic properties.
7. Lubrication zone (contact area) wider than the thickness of the poro-elastic material.
8. Negligible surface roughness.
9. Constant temperature.

B. Governing equations

Under hypothesis 4, 5 and 8 and assuming values of the Poisson coefficient (v) of the deformable material slightly lower than 0.5, the deformation (δ) depends only on the local pressure (P). This relationship is expressed by the *column model* (Eq. 1) [5], in which E'' is the equivalent elastic modulus, E is the elastic modulus and L is the thickness of the elastic material.

$$\delta = \frac{L}{E''} P;\ E'' = \frac{(1-\nu)E}{(1+\nu)(1-2\nu)} \tag{1}$$

In a hypotetical, non-deformed state, the thickness of the lubrication channel is given by the distance between a plane

surface and the surface of the equivalent sphere, that is approximated by the closest paraboloid (see Fig.1); the separation at the point of closest proximity between both surfaces is H0 (which can be greater or less than zero, depending on the acting load). The equation of the actual channel shape *(H,* see Eq. 2) is obtained by adding the deformation that prevents indentation (if $H_0 < 0$) of the metallic component into the UHMWPE component.

$$H = H_0 + \frac{X^2}{2R} + \frac{Y^2}{2R} + \delta \qquad (2)$$

The volume of exuded or absorbed fluid by the porous elastic material depends on its deformation and *exudation factor* θ, the latter measures the ability of a porous material to absorb or exude fluid from its surface and it can be quantified from compaction tests [3]. Applying the mass and momentum balances under the hypothesis 1-3 in a small volume of synovial fluid in a representative region of the channel, a modified 2D-Reynolds lubrication equation (Eq. 3) [6] is obtained.

$$\frac{\partial}{\partial X}\left(\frac{H^3}{12\mu}\frac{\partial P}{\partial X}\right) + \frac{\partial}{\partial Y}\left(\frac{H^3}{12\mu}\frac{\partial P}{\partial Y}\right) = \frac{\partial}{\partial X}(VH - 2V\delta\theta) \qquad (3)$$

The shape of the lubrication channel and the pressure distribution are symmetric with respect to the *x-z* plane [5], so the considered domain is only a half of the real domain. Fig. 2 shows the considered domain and the applied boundary conditions.

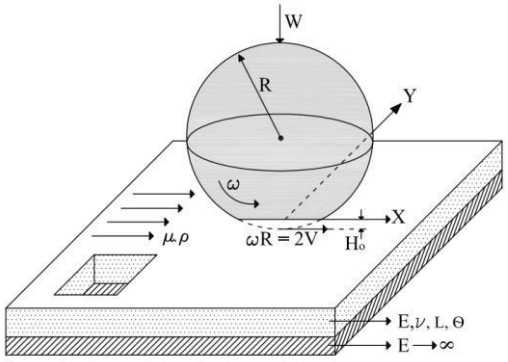

Fig. 1 Equivalent geometry of hip prostheses for loaded contact.

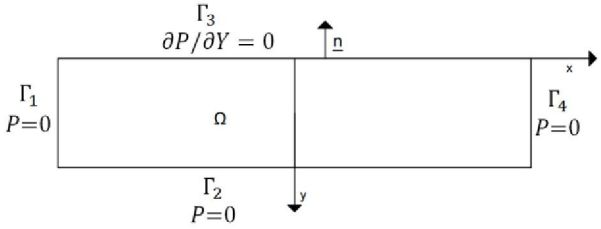

Fig. 2 Considered domain (half of the total domain) and boundary conditions applied.

Therefore, the load W is a half of the total applied load and it must be equilibrated by the fluid pressure distribution to avoid the solid contact (Eq. 4).

$$W = \int_\Omega P\, dX\, dY \qquad (4)$$

With the aim of representing multiple dimensional situations and to assure the convergence of the algorithm, the dimensionless form of equations (1)-(4) was obtained by scaling with the characteristic magnitudes defined in table 1. Equation (1)-(3) become

$$\frac{\partial}{\partial x}\left(h^3\frac{\partial p}{\partial x}\right) + \frac{\partial}{\partial y}\left(h^3\frac{\partial p}{\partial y}\right) = \frac{\partial}{\partial x}[(NG)h - (NE_1)\theta p] \qquad (5)$$

$$h = h_0 + x^2 + y^2 + \delta \qquad (6)$$

$$\delta = NE_2 p \qquad (7)$$

while Ec. 4 remains unchanged.

C. Solution technique

A computational code based on the finite element method, Newton's method and parametric continuation, was used in order to solve the equations. The numerical scheme is described in detail in [6]. Pressures in each node are the only unknowns since deformations are considered as im-

Table 1 Characteristic magnitudes and numbers for the definition of dimensionless variables.

	Characteristic magnitude
Characteristic pressure	$(\mu_0 V/L)\sqrt{2R/L}\ 10^5$
Characteristic length in X and Y direction	$\sqrt{2RL}$
Characteristic length for channel height	L
Characteristic flow rate	2VL
Characteristic load	$\mu V\ 2R\sqrt{2R/L}\ 10^5$
Scale constant	$NG = 12.10^{-5}$
Elastic number 1	$NE_1 = \frac{24\mu V\sqrt{2R/L}}{E''L}$
Elastic number 2	$NE_2 = NE_1/(24 \cdot 10^{-5})$

Table 2 Physical and operatives parameters of a hip prosthesis.

Symbol	Value	
R	0,35 m	Equivalent sphere radius
V	0,02 m/s	Average tangential speed of the spherical surface
μ	1,0 Pa s	Viscosity at channel input
E	$20\ 10^6$	Elastic modulus of the porous material
ν	0,4	Poisson coefficient of the porous material
L	$1\ 10^{-3}$ m	Porous material thickness

plicit functions of pressure.

The domain was discretized with nine nodes rectangular elements, so the unknown function is approximated by biquadratic shape functions. The direction of relative motion (*x*-direction) is the main direction over which friction occurs; therefore, there are more elements along it. In order to minimize the oscillations observed in preliminary results, refinements were made at channel exit. Hereafter, *90x20* mesh will refer to the discretization that contains 90 elements along the *x*-direction and 20 elements along the *y*-direction. The same convention was taken for the *140x25* mesh.

Then equations (5)-(6) were solved for physical and operative parameters of a hip prosthesis (Table 2). Finally, the friction factors ϕ_i $(i = 1, 2)$ were calculated. These are defined as the ratio between frictional force $(f_i, i = 1,2)$ and the applied load (Eq. 8). The frictional forces are obtained by integrating the shear stresses on both surfaces of the contact: index 1 stands for the polymer surface and index 2 for the femoral component surface.

$$\phi_i = \frac{f_i}{w} \tag{8}$$

III. Results and Discussion

Figure 3 shows a section (*y=0*) of the channel shape for both meshes and it can be observed how results depend on discretization. Particularly, the amplitude of the oscillations at the channel exit is reduced by increasing the number of elements. As was established in the one-dimensional analogue problem, these oscillations could be due to the order of the Reynolds equation and the imposed boundary conditions [7]. The limited computational resources do not allow the use of more refined meshes. In what follows we only discuss the results obtained with the 140x25 mesh.

The great deformation of the low stiffness material analyzed, assures a better distribution of load (Fig. 4) and also the formation of a thicker lubrication channel. The acetabular component is typically made of UHMWPE whose elastic modulus exceeds 500 MPa and the yield stress is approximately 21 MPa [8]. Nevertheless, a 5 MPa tension is usually taken as an acceptable design criterion in terms of fatigue failures that may happen in the material. The maximum pressure obtained (Fig. 4) considering the parameters of Table 2, are lower than 4 MPa thus the material yield stress would not be exceeded.

When the load increases by a factor of 2.13 (Fig. 5), the positive pressure increases in the entire domain and there is also a 30% decrease of the ratio between the maximum subambiental and the maximum positive pressures. Even though subambiental pressures do not appear in natural joints, they are predicted for the model due to the imposed boundary conditions (Sommerfeld conditions). The Reynolds boundary conditions, which best represent reality, involve the determination of an unknown (free) boundary by specific methods which justify further work.

The comparison between the curves for a load of 222 N in Fig. 5 shows an increased channel height in the central area and also the occurrence of oscillations at its exit, both due to the increased exudation factor of the elastic material. The pressure distribution, meanwhile, is practically not influenced by the effects of the exudation and absorption process.

The channel height at *x=y=0* (h_0) increases linearly as the exudation factor augments (Fig. 6). Furthermore, Fig. 6 shows how the minimum channel height h_{min} (located at the exit) diminishes when the exudation factor increases. The limited computational resources do not allow obtaining results for higher exudation factors; nevertheless if this behavior persists a maximum exudation factor is expected, due to the possible solid to solid contact in the h_{min} region.

The lack of a good lubrication condition in artificial joints results in high friction coefficients (0.06-0.08) [9] when compared with those of natural joints (0.001-0.01) [10]. Fig. 7 illustrates the decrease of the friction coefficient on the polymeric material when the exudation factor in-

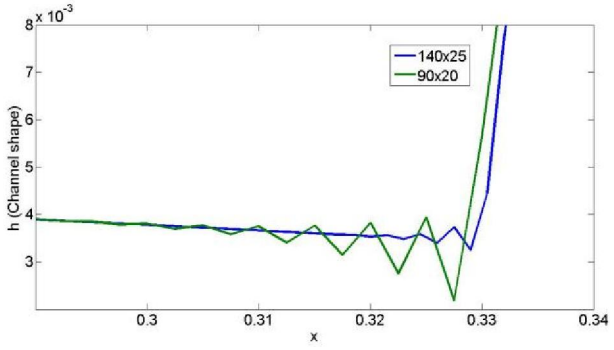

Fig. 3 Channel shape at its exit, for both discretizations and $\theta = 0.01$.

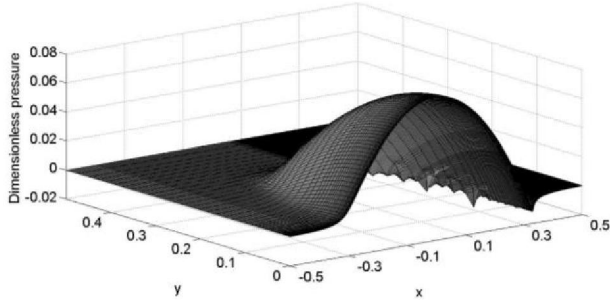

Fig. 4 Pressure distribution in half of the total domain for *E=20 MPa*, $\theta = 0.01$ and 140x25 mesh.

creases. This suggests that the phenomenon of fluid exudation and absorption not only improves lubrication by the self-lubricating effect, but would also be directly responsible for the low friction in natural joints. These features could be considered in the design of future prostheses.

IV. Conclusions

Even though the solution of the two-dimensional lubrication model presented depends on the specific modified Reynolds equation used, the information provided by this model is extremely difficult to obtain by experimental methods [1].

The deformability of a low stiffness and porous material as the one analyzed here, contributes to the elasto-hydrodynamic lubrication and assures a better load distribution, thus the normal stresses that cause material fatigue are reduced, as happens in healthy natural joints. Moreover, the exudation could reduce wear by reducing the friction factor.

The prediction of subambient pressures and oscillations at the channel exit shows the need of more realistic boundary conditions and the use of more refined discretizations, which motivates future work.

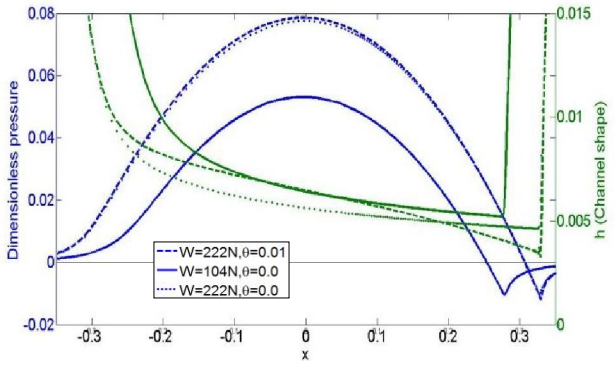

Fig. 5 Pressure distribution (blue) and channel shape (green) in the *x-z* plane for *y=0*, for two loads, two exudation factors and 140x25 mesh.

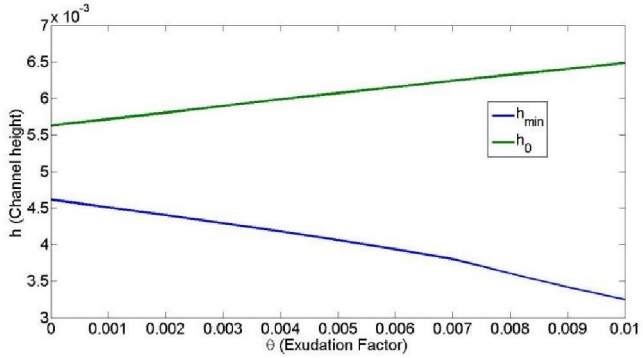

Fig. 6 Minimum channel height h_{min} (blue) and channel height h_0 at *x=y=0* (green) versus exudation factor for the 140x25 mesh.

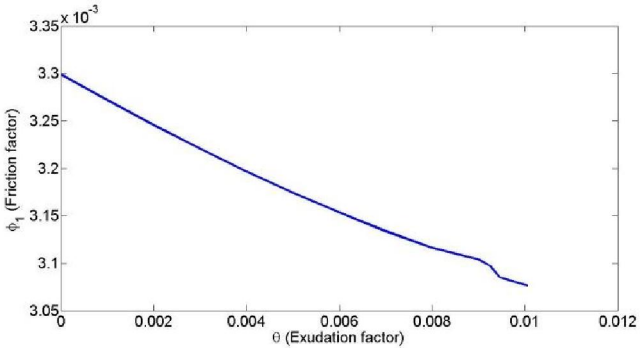

Fig. 7 Friction coefficient on polymeric surface versus the exudation factor, for 140x25 mesh.

Acknowledgment

To Universidad Nacional de Entre Ríos for its financial support by PID 6123. B.A. Weiss acknowledges partial support from a PhD fellowship from CONICET.

Conflict of Interest

There is no conflict of interest.

References

1. Mattei L, Di Puccio F, Piccigallo B, Ciulli E (2011). Lubrication and wear modeling of artificial hip joints: A review. Tribol Int 44(5):532-549.
2. Bozic K, Kurtz S, Lau E, Ong K, Vail T, Berry D (2009). The Epidemiology of Revision Total Hip Arthroplasty in the United States. J Bone Joint Surg Am, 91(1):128-33.
3. Di Paolo J, Berli M (2006) Numerical analysis of the effects of material parameters on the lubrication mechanism for knee prosthesis. Comput Methods Biomech Biomed Engin 9(2):79-89.
4. Berli M, Campana D, Ubal S, Di Paolo J (2009) Lubrication model of a knee prosthesis, with non Newtonian fluid and porous rough material. Latin Am Appl Res 39(2):105-11.
5. Jin ZM, Dowson D, Fischer J (1993) Fluid film lubrication in natural hip joints. Thin films in Tribology 25:545-555.
6. Di Paolo J, Berli M (2002) Análisis por elementos finitos de un modelo de lubricación 2D para una prótesis de cadera. Mec. Computacional 21:2440-2455.
7. Di Paolo J, Corvalán C, Saita F (1995) Solución numérica de la ecuación de Reynolds. Formulación diferencial vs formulación integral. Rev. Int. Mét. Num. Cál. Disg. Ing. 11(3):303-322.
8. Lee K, Pienkowsi (1998) Viscoelastic recovery of creep-deformed Ultra-High Molecular Weight Polyethylene (UHMWPE). Characterization and properties of Ultra-High Molecular Weight Polyethylene, ASTM STP 1307, Gsell R, Stein H, Ploskonka J, Eds. pp 30-36.
9. Jin ZM, Stone M, Ingham E, Fisher J (2006) Biotribology. Current Orthopaedics 20:32-40.
10. Ermakov SF (1993) Biomechanics of synovia in living joints. 1. Modern concepts of living joints frictions, wear and lubrication. J Friction and Wear, 14(6):97-109.